2019 IEEE International Ultrasonics Symposium (IUS)
Glasgow, Scotland, October 6-9, 2019

Non-Contact Thermoacoustic Sensing and Characterization of Plant Root Traits

Ajay Singhvi*, Bo Ma*, Johannes Daniel Scharwies†,
José R. Dinneny†, Butrus T. Khuri-Yakub*, and Amin Arbabian*
*Department of Electrical Engineering, Stanford University †Department of Biology, Stanford University
Stanford, CA, USA

***Abstract*—Measuring below-ground plant and soil traits such as root biomass, water distribution, and soil compaction is of high interest to plant breeders and agronomists alike. However, there are limited technologies available that can sense these traits. Current methods for sensing roots are either invasive or not readily field deployable. Thus, we propose a novel non-contact thermoacoustic sensing system that can be used to characterize roots in a high-throughput, non-invasive and non-destructive fashion. Upon microwave excitation, the dielectric contrast between roots and soil generates an ultrasound signal via the thermoacoustic effect. Detection of the ultrasound signal in air is achieved using highly sensitive capacitive micromachined ultrasonic transducers with minimum detectable pressures as low as 278 μPa_{RMS}, in order to overcome the large interface loss due to the impedance mismatch at the soil-air boundary. In this paper, we demonstrate a system that can detect agarose-based root phantoms in two different soil types. A linear-regression mapping of the received thermoacoustic data to properties like soil water content, root osmotic potential and root size shows excellent correlation, with R^2 greater than 0.9 in all cases.**

***Index Terms*—capacitive micromachined ultrasonic transducer, CMUT, ultrasound imaging, non-contact microwave-induced thermoacoustics, below-ground sensing**

I. Introduction

Advances in crop breeding and significant improvements in agricultural practices have led to improved global crop productivity over the past decades. However, crop yields are in danger of stagnating [1]. While previous breeding and management efforts have largely focused on above-ground plant traits, below-ground plant and soil traits have a significant potential for improving crop yields and the environment [2]. The availability of extensive high-quality below-ground data could be used to develop new root-focused cultivars with enhanced root systems to improve crop yields and aid long-term soil carbon storage for increasing soil humus levels and removal of atmospheric carbon dioxide [3]. Furthermore, continuous monitoring of soil salinity and soil moisture content [4] could improve soil health by intelligent, targeted and efficient use of fertilizers and better irrigation scheduling.

A primary obstacle in doing so is the lack of robust, field-deployable plant phenotyping tools. This is especially true for sensing below-ground parameters like soil moisture and salinity, root biomass as well as root system architecture [5].

This work was supported by Advanced Research Projects Agency-Energy Grant DE-AR0000825, sponsored by the ROOTS program.

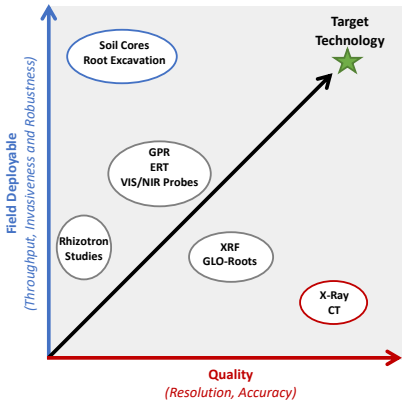

Fig. 1. Survey of currently available below-ground sensing methods. CT: Computed Tomography, ERT: Electrical Resisitivity Tomography, GPR: Ground Penetrating Radar, GLO-Roots: Growth and Luminescence Observatory for Roots, XRF: X-Ray Fluorescence.

As seen from Fig. 1, current approaches to root phenotyping are either lab-based technologies that are high-resolution (X-Ray, CT, GLO-Roots, rhizotrons) with lower throughput and poor translation to the production setting, or field-based techniques that are lower resolution (GPR, ERT), destructive (root excavation), and low-throughput (in-situ root imagers, soil cores) but generate more relevant data. Additionally, most existing approaches are invasive, in that, they require the addition of probes, sensors or other specialized structures into the soil or on the plant. GPR systems are currently the gold-standard when it comes to non-invasive, non-destructive below-ground sensing but they have a fundamental tradeoff between resolution and depth penetration through the operating frequency, and can only operate reliably in regions with electrically resistive soil [6].

We propose a non-contact thermoacoustic phenotyping solution that is a powerful hybrid of microwave and ultrasound sensing modalities [7], combining the good dielectric contrast of microwave imaging and the high resolution of ultrasound. Non-contact ultrasound (US) detection eliminates the difficult problem of achieving mechanical coupling at the irregular soil surface and significantly increases system flexibility. Moreover, it goes one step beyond non-invasive methods by eliminating operator dependence, thereby enabling high-throughput, minimal supervision imaging and opening the door for fully autonomous imaging employing commercial drones or other vehicles. The proposed system also allows

978-1-7281-4596-9/19/$31.00 ©2019 IEEE

for dynamic measurements of a number of underground traits. Unlike GPR, the multi-modal nature of the proposed system mitigates the depth-resolution tradeoff by completely decoupling the excitation and detection schemes and provides multiple degrees of freedom in system design. It can thus can potentially be employed without major limitations on soil types or other conditions, which in turn allows for highly adaptable, optimized solutions for any use case.

II. System Overview

A. Thermoacoustic Physics

The thermoacoustic (TA) effect describes the generation of pressure due to differential heating at interfaces with dielectric contrast when exposed to microwave excitation. The generation and propagation of this TA pressure is governed by the following equation

$$\left(\nabla^2 - \frac{1}{v_s^2}\frac{\partial^2}{\partial t^2}\right) p(\boldsymbol{r},t) = -\frac{\beta}{C}\frac{\partial Q(\boldsymbol{r},t)}{\partial t}. \tag{1}$$

where v_s is the speed of sound, $p(\boldsymbol{r},t)$ is the generated pressure at position $\boldsymbol{r}$ and time t, β is the thermal expansion coefficient, C is the specific heat capacity, and $Q(\boldsymbol{r},t)$ is the heating function. The heating function $Q(\boldsymbol{r},t)$ is given by the equation below

$$\begin{aligned} Q(\mathbf{r},t) = \sigma(\mathbf{r})|\boldsymbol{E}(\mathbf{r},t)|^2 + 2\pi f\epsilon''(\mathbf{r})|\boldsymbol{E}(\mathbf{r},t)|^2 \\ +2\pi f\mu''(\mathbf{r})|\boldsymbol{H}(\mathbf{r},t)|^2 \end{aligned} \tag{2}$$

Based on equation (2), at each point $\mathbf{r}$, $Q(\boldsymbol{r},t)$ depends on the microwave excitation frequency f, the root-mean squared magnitudes of the electric and magnetic fields $|\boldsymbol{E}|$ and $|\boldsymbol{H}|$, the conductivity σ, the complex electric permittivity ϵ'' and the complex magnetic permeability μ'' of the absorbing media.

The microwave excitation source, and hence the absorbed EM energy is modulated at the US frequency of interest, in order to generate a TA pressure signal that can be captured using a matched US transducer. A challenge with non-contact US detection in the proposed system is the large interface loss that occurs as the US signal travels from one medium to another due to their impedance mismatch. We overcome this loss in signal by using highly sensitive capacitive micromachined ultrasound transducers (CMUTs) that can be designed to have a good balance between sensitivity and bandwidth.

B. Concept of Operation

A conceptual diagram of the proposed system is shown in Fig. 2, wherein a modulated microwave excitation source heats the roots and the soil, creating a pressure signal at their interface due to differential heating resulting from varying amounts of water and salts present in the roots and surrounding soil. [8] and [9] measure the dielectric properties of different types of soil and plant roots and show sufficient dielectric contrast for TA signal generation at the root-soil interface as per equation (2).

Once the US signal is generated at the root-soil interface, it propagates through the soil and across the soil-air interface, at a propagation speed and with attenuation and interface loss that depend on the soil composition in terms of air pores, moisture content and particle size [10]. As the US signal travels across the soil-air interface, it is then captured using CMUTs present at a standoff in air.

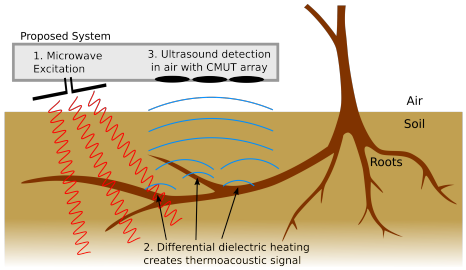

Fig. 2. Conceptual view of proposed thermoacoustic sensing system.

III. Experimental Design

A. Microwave Excitation Unit

The generated TA signal depends on the microwave frequency as well as the dielectric properties at that microwave frequency, as seen in equation (2). Thus, the microwave excitation frequency should be chosen to maximise the differential heating between the roots and soil. However, there are also practical limitations to the upper bound of the microwave excitation frequency, since the penetration depth through soil is limited for higher frequencies. Based on these trade-offs and available high-power microwave sources, we choose to operate at a microwave frequency of 2.7 GHz with a 2 kW peak power (average power limited to 7 W).

B. Air-coupled CMUT receiver

As discussed in Section II, a major challenge for non-contact operation of the TA system is the frequency-dependent US losses [10] as the generated signal travels through the soil (attenuation in soil), propagates from the soil to air (interface loss due to large impedance mismatch) and finally propagates in air to the airborne CMUT receiver. The US frequency chosen also governs the resolution of the non-contact TA system [7]. Achieving cm-scale detection resolution with large standoffs in air (> 20 cm) while obtaining reasonable signal-to-noise ratio for high detection confidence requires operation at US frequencies in the 100 kHz range as higher frequencies are prohibitively attenuating.

The CMUTs used in these experiments are capacitive US sensors made of a thin vibrating plate over a vented cavity, which introduces squeeze film losses that allow optimization of the CMUT design to achieve the desired sensitivity, while maximizing achievable bandwidth. The CMUT has a center frequency of 71 kHz, with a 3.5% fractional bandwidth or a quality factor of 28. The CMUT interfaced with a single-stage resistive feedback trans-impedance amplifier (gain of 15 $M\Omega$) as an analog front-end, has an experimentally measured minimum detectable pressure of 278 μPa_{RMS}.

The frequency of the generated TA signal depends on the envelope of the excitation signal and should be in the CMUT

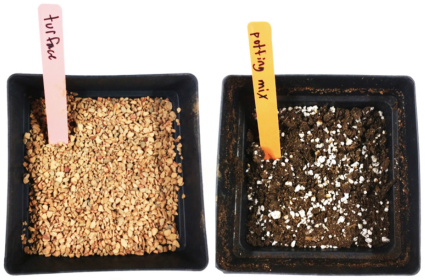

Fig. 3. Soil types used in experiments: Turface (left) and Potting Mix (right).

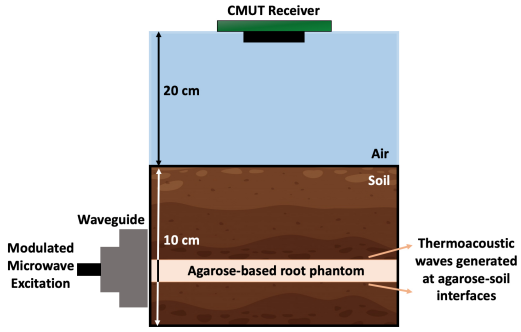

Fig. 4. Schematic diagram of experimental setup showing an open-ended waveguide providing microwave excitation which creates TA signals at the phantom-soil interface that are captured using CMUT receivers in air.

operating frequency range. To enable this, the microwave signal at 2.7 GHz is modulated using a pulse train (in this case, 10 cycles) with a frequency of 71 kHz, equal to the center frequency of the CMUT and a 50% duty cycle. Additional details regarding the same can be found in [7].

C. Soil and Root Selection

We choose two contrasting artificial soil types for the experiments – Turface (TURFACE MVP, PROFILE Products LLC) and Potting Mix (PRO-MIX HP, Premier Tech Horticulture) as seen in Fig. 3. The soil selection was done to have a mix in terms of soil granularity, compactness, water retention capacity and use cases. Turface is an inorganic, calcined, non-swelling illite clay that is used as a soil conditioner and has large grain sizes and high porosity. Potting Mix is an artificial soil composed of sphagnum peat moss $(65-75\%)$, perlite $(8-35\%)$, limestone and a wetting agent. It is commonly used to grow plants in greenhouses and has a fine structure and high organic content resulting in higher water holding capacity.

Given that this is the first demonstration of a thermoacoustic root-sensing system, we choose to use agarose-based root phantoms that mimic properties of biological plant materials. This allows for tighter control over parameters of interest and also makes possible repeatable measurements which enable robust mapping of TA signals to root and soil parameters. The agarose-based root phantoms were synthesized using modified versions of established procedures [11] to match ultrasonic and dielectric properties of typical root structures [9]. Ultrasonic properties of the phantoms were tested using calibrated pitch-catch measurements, while dielectric properties at the microwave frequency of interest were measured using a dielectric probe kit and Vector Network Analyzer. Fig. 4 shows a schematic of the experimental setup used.

D. Parameters of Interest

We focus on three parameters of interest in experiments - soil water content, root size, and root osmotic properties. The soil or the agarose based root-phantoms shown in Fig. 4 were treated in a controlled manner to change only the specific parameter under study. The sample was then excited using the microwave excitation scheme discussed earlier, and A-scan TA signals were captured. This data was further processed to extract characteristics like signal time of arrival, inter-echo time and amplitude in order to map them to parameters of interest. Typically collected A-scan data is shown in Fig. 5.

IV. Results and Discussion

Fig. 6 shows a selection of results, both raw A-scan TA data captured during experiments, as well as a linear regression mapping of extracted signal characteristics to root or soil parameters of interest.

First, experiments were run to determine changes in TA signals with change in soil water content, wherein dry soil was incrementally watered until it was saturated at 100% of its water retention capacity. As seen in Fig. 6(a), the amplitude of the signal of interest decreased with increase in soil water content. This can be attributed to lower dielectric contrast between the root and soil as water content increases, resulting in lower TA pressures being generated. It can also be observed that the signal of interest arrives earlier in wetter soil, which is due to an increase in the US speed in soil with increasing moisture content [10].

Next, agarose-based phantoms with varying salt content were created to assess the effect of changes in osmotic properties. Fig. 6(b) shows an increase in signal amplitude as the phantom salt concentration, or in other words, root osmotic potential increased. These results match expectations, since the measured dielectric loss of the phantoms increases with increasing salt content, causing larger TA signal generation.

Lastly, to sense changes in root size, agarose based phantoms of different sizes were created and experiments run as shown in Fig. 4. As the root size increased, it was seen that the difference in time between TA signals arriving from the top and bottom root-soil interfaces also increased due to the longer path length traversed. We quantified this as a change in

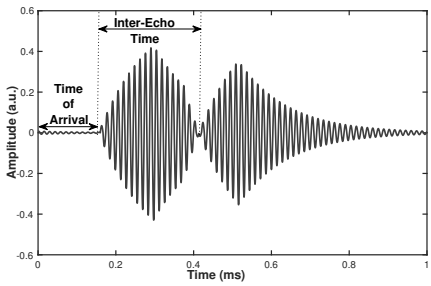

Fig. 5. Typical thermoacoustic A-scan data collected during experiments.

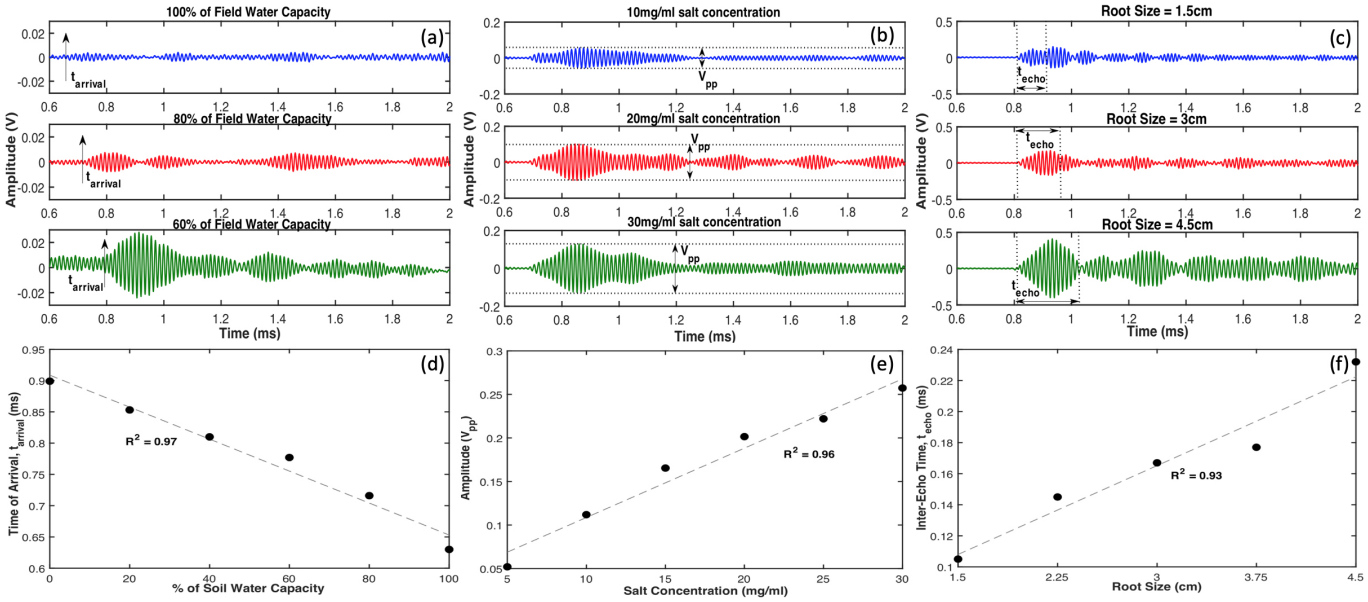

Fig. 6. Thermoacoustic A-scan data and mapping of signal characteristics to parameters of interest - (a), (d) soil water content (b), (e) root salt concentration and (c), (f) root size. By default, experiments were run in dry soil (Turface), with a root phantom 1.5 cm in size, with 10mg/ml salt concentration.

the inter-echo time as seen in Fig. 6(c). We then performed a linear regression mapping by choosing unique characteristics of the A-scan data that change with the parameters of interest, as shown in Fig. 6(d)-(f). Wherever possible, the signal characteristics extracted were time-based properties since they provide robust metrics that can be easily decoupled to map to a single parameter of interest. TA mapping shows a coefficient of determination, $R^2 > 0.9$ for all the three parameters being sensed - for all the three parameters being sensed - soil water content, root phantom size and root osmotic properties.

In order to demonstrate TA root detection feasibility, we ran experiments with root phantoms buried $10\ cm$ deep in soil. TA signals were detected with an SNR of $4.9\ dB$ and $7.8\ dB$ through Potting Mix and Turface, respectively. If the system is assumed to be coherent, with a non-fluctuating target, it provides a detection probability greater than 85% through $10\ cm$ of Potting Mix and greater than 95% through $10\ cm$ of Turface when assuming a 10% false alarm rate.

V. Conclusion

In this paper, we demonstrate the first non-contact thermoacoustic below-ground sensing system that can accurately measure soil moisture content, the size of an agarose-based root phantom and its osmotic properties. The entire system can potentially operate without contact in a non-invasive and non-destructive fashion, paving the way for dynamic, high-throughput measurements in the field. Future work includes extending experiments to plant materials instead of phantoms, as well as demonstrating improved system capabilities in terms of detection sensitivity and resolution by using CMUTs with improved sensitivity [12] and operating at multiple frequencies.

References

[1] D. K. Ray, N. Ramankutty, N. D. Mueller, P. C. West, and J. A. Foley, "Recent patterns of crop yield growth and stagnation," *Nature communications*, vol. 3, p. 1293, 2012.

[2] J. Lynch, "Root architecture and plant productivity." *Plant physiology*, vol. 109, no. 1, p. 7, 1995.

[3] K. Paustian, N. Campbell, C. Dorich, E. Marx, and A. Swan, "Assessment of potential greenhouse gas mitigation from changes to crop root mass and architecture," Booz Allen Hamiltion Inc., McLean, VA (United States), Tech. Rep., 2016.

[4] N. Yan, P. Marschner, W. Cao, C. Zuo, and W. Qin, "Influence of salinity and water content on soil microorganisms," *International Soil and Water Conservation Research*, vol. 3, no. 4, pp. 316–323, 2015.

[5] H. F. Downie, M. Adu, S. Schmidt, W. Otten, L. X. Dupuy, P. White, and T. A. Valentine, "Challenges and opportunities for quantifying roots and rhizosphere interactions through imaging and image analysis," *Plant, cell & environment*, vol. 38, no. 7, pp. 1213–1232, 2015.

[6] J. A. Doolittle, F. E. Minzenmayer, S. W. Waltman, E. C. Benham, J. Tuttle, and S. Peaslee, "Ground-penetrating radar soil suitability map of the conterminous united states," *Geoderma*, vol. 141, no. 3-4, pp. 416–421, 2007.

[7] A. Singhvi, K. C. Boyle, M. Fallahpour, B. T. Khuri-Yakub, and A. Arbabian, "A microwave-induced thermoacoustic imaging system with non-contact ultrasound detection," *IEEE transactions on ultrasonics, ferroelectrics, and frequency control*, 2019.

[8] W. E. Patitz, B. C. Brock, and E. G. Powell, "Measurement of dielectric and magnetic properties of soil," Sandia National Labs., Tech. Rep., 1995.

[9] T. Ellis, K. Feher, W. Murray, K. Paul, J. Brophy, K. Jacobsen, V. Koul, P. Leppert, and J. Smith, "Electrical measurement of root mass and root location," *Rural Industries Research and Development Corporation. Canberra: Australia*, pp. 1–32, 2008.

[10] M. L. Oelze, W. D. O'Brien, and R. G. Darmody, "Measurement of attenuation and speed of sound in soils," *Soil Science Society of America Journal*, vol. 66, no. 3, pp. 788–796, 2002.

[11] D. Oliveira, T. Santos, L. Maggi, and R. Costa-Felix, "Ultrasound propagation velocity and acoustic attenuation on agarose phantoms' in three different manufacture techniques," in *2014 Pan American Health Care Exchanges (PAHCE)*. IEEE, 2014, pp. 1–3.

[12] B. Ma, K. Firouzi, K. Brenner, and B. Khuri-Yakub, "Wide bandwidth and low driving voltage vented cmuts for airborne applications," *IEEE transactions on ultrasonics, ferroelectrics, and frequency control*, 2019.